Agricultural and Forest Meteorology 203 (2015) 142–157

Contents lists available at ScienceDirect

Agricultural and Forest Meteorology

journal homepage: www.elsevier.com/locate/agrformet

Snowpack-climate manipulation using infrared heaters in subalpine forests of the Southern Rocky Mountains, USA

Leah Meromy[a], Noah P. Molotch[b,c,*], Mark W. Williams[b], Keith N. Musselman[d], Lara M. Kueppers[e]

[a] Institute of Arctic and Alpine Research, University of Colorado at Boulder, Boulder, CO, United States
[b] Department of Geography, Institute of Arctic and Alpine Research, University of Colorado at Boulder, Boulder, CO, United States
[c] Jet Propulsion Laboratory, California Institute of Technology, Pasadena, CA, United States
[d] University of Saskatchewan, Saskatoon, Canada
[e] Sierra Nevada Research Institute, University of California, Merced, CA, United States

ARTICLE INFO

Article history:
Received 11 July 2014
Received in revised form
23 December 2014
Accepted 29 December 2014
Available online 20 January 2015

Keywords:
Snow
Subalpine
Modeling
Climate change
Climate manipulation experiment
IR heaters

ABSTRACT

Effects of infrared heaters on snow accumulation, snowmelt, and snow–atmosphere energy exchange were examined at Niwot Ridge, Colorado (CO) and compared to a naturally warmer, but otherwise similar subalpine site in the Valles Caldera National Preserve, New Mexico (NM). Observed snow accumulation was 30% lower on average and snow melted out 16 days earlier in the heated plots compared to the controls. Soil temperature during snowmelt was 3 °C greater on average and soil moisture was 4% lower on average in heated plots compared to controls. In NM, snow accumulation was 23% lower, snow melted 23 days earlier, soil temperature was 0.6 °C greater, and soil moisture was 13% lower on average relative to CO controls. In order to estimate differences in energy and mass balance fluxes at the snow–atmosphere interface in control versus warmer plots, the 1-D, physically based snowmelt model, SNOWPACK, was used. Model results indicated that heaters alter radiative, turbulent and mass fluxes by amounts comparable to the differences between CO and NM fluxes. The proportion of the energy flux associated with latent heat exchange during snowmelt was 9–27% of the total energy flux in heated models and 19–22% of NM models compared to 3–7% in control models. Thus, sublimation loss to the atmosphere was greater in both experimentally and naturally warmer cases relative to the control case. We conclude that IR heaters can provide alterations to the timing and magnitude of snow accumulation and snowmelt consistent with conditions observed at a warmer analog site and with climate and hydrology model projections. Impacts of IR heating on energy partitioning and sublimation should be considered when designing manipulations of the snowpack, as reductions in snowmelt water may alter biological or ecological processes.

1. Introduction

Global mean surface temperature is projected to increase by 1.5–4 °C by the end of the 21st century with wide-ranging impacts (Stocker et al., 2013). Ecosystems in seasonally snow-covered regions will be subjected to substantial changes in climate conditions, as even subtle changes in temperature can alter precipitation type, and the timing of snow accumulation and snowmelt (Bales et al., 2006). Such changes are especially difficult to quantify in mountainous regions of complex topography (Lundquist and Flint, 2006) and high interannual variability (Pagano and Garen, 2005).

Climate manipulation experiments increasingly have been used to study potential ecological consequences of climate change (Wu et al., 2011). Climate manipulations in seasonally snow-covered regions have included snow fences to manipulate snow depth (Loik et al., 2013; Williams et al., 1998a,b), shoveling to change snow depth or snow cover duration (Dunne et al., 2003; Decker et al., 2003; Comerford et al., 2013), and open top chambers (OTCs) to passively warm the soil (Wipf and Rixen, 2010). Active climate manipulation using aboveground thermal infrared (IR) radiation to warm experimental plots is an attractive method because one can directly manipulate surface energy inputs with few methodological limitations (Harte et al., 1995; Kimball et al., 2008; Aronson and McNulty, 2009).

* Corresponding author at: Institute of Arctic and Alpine Research, University of Colorado, Boulder, Campus Box 450 UCB, Boulder, CO 80309, United States. Tel.: +1 303 492 6151.
E-mail addresses: leah.meromy@colorado.edu (L. Meromy), noah.molotch@colorado.edu (N.P. Molotch), markw@snobear.colorado.edu (M.W. Williams), keith.musselman@usask.ca (K.N. Musselman), lkueppers@ucmerced.edu (L.M. Kueppers).

http://dx.doi.org/10.1016/j.agrformet.2014.12.015
0168-1923/

In snowmelt-dominated systems this is beneficial as one can manipulate rates of snowmelt and the timing of snow disappearance without disruptive soil or snow manipulation. Several studies have used overhead infrared heating in snow-dominated ecosystems (Harte et al., 1995; Wan et al., 2002; Auyeung et al., 2013; Moyes et al., 2013), and have reported increases in soil temperature of 1–2 °C during the growing season, with higher temperatures closer to the surface and under higher heater intensities. In these studies, heating also decreased growing season soil moisture, advanced the timing of snowmelt and/or reduced snow depth and the frequency of freeze–thaw events. However, detailed assessments of the impacts of IR heaters on the snowpack have not been conducted.

IR heating is considered one of the most realistic methods for simulating a warmer climate as it causes minimal physical disruption to an ecosystem, has moderate temperature variability, and can be applied in a variety of environmental conditions (Aronson and McNulty, 2009). However, infrared heating falls short of exactly replicating a warmer climate because it does not directly warm the air, but instead warms the land surface, and does not maintain relative humidity (Amthor et al., 2010). While this latter critique is based on an understanding of basic principles of heat transfer, one study found that IR heaters can, in fact, cause increases in minimum and mean air temperatures (Wan et al., 2002). Regardless of whether or not IR heaters warm the surface and not the air, IR heaters raise canopy and soil temperatures as would be expected with global warming (Kimball, 2011), and thus remain a useful method for studying ecosystems in the context of global warming.

When used to alter winter climate, growing season length, and/or the timing of snowmelt, it is necessary to consider effects and artifacts associated with this approach. For example, unless continuously adjusted, the impact of changes in snow depth alters the height of the heaters with respect to the snow surface and therefore alters energy transfer efficiency and the spatial footprint of energy inputs to the surface in the same manner as a growing crop canopy (Wall et al., 2011). In addition, the snow surface is an evolving medium in which IR heating can increase the rate of snow metamorphism and increase snow surface grain size. As a result, snow-surface albedo would decrease and absorption of shortwave radiation would increase (Flanner et al., 2011). Infrared heaters may also alter turbulent exchange between the snow and the atmosphere as the snow surface temperature cannot exceed 0 °C. Hence, if the snowpack warming is considerable, then the sign of the temperature gradient between the snow and the atmosphere may reverse as the snow surface temperature becomes greater than the air temperature (Molotch et al., 2007). In some instances, partitioning of available energy to latent heat fluxes may be increased by infrared heaters, resulting in increased sublimation and reduced snowmelt and soil–water inputs.

Detailed analysis of snowpack changes within the IR heater footprint may also improve understanding of snowpack response to climate warming. Given the importance of the snowpack to winter soil temperature, soil moisture, and light availability, future changes in snowpack conditions may have significant ecological impacts (Brooks et al., 2011; Campbell et al., 2005) Recent work has highlighted the multi-decadal decline in snow accumulation in Earth's mountainous regions (Hamlet et al., 2005; Mote et al., 2005). Mote et al. (2005) found snow water equivalent (SWE) decreases of 2–30% throughout the western US from observed SWE records spanning 1950–1997. Additionally, the timing and magnitude of snowmelt pulses are sensitive to anticipated future changes in climate (Adam et al., 2009). For example, projections indicate that the period of snow cover in the Rocky Mountains may decrease by 1–3 months by the end of the century, and maximum SWE values may decline by an average of 40% (Rasmussen et al., 2014; Deems et al., 2013). These potential changes in snowmelt have profound ecological implications as the magnitude of snowpack and timing of snowmelt strongly influence forest growth (Trujillo et al., 2012), fire regimes, (Westerling et al., 2006) and soil respiration rates (Monson et al., 2006). IR heaters may be well suited for evaluating the potential ecological impacts of reduced snow cover duration and SWE. However, precipitation predictions are highly uncertain and IR heaters are of limited value for evaluating scenarios of precipitation change.

In addition to changes in timing and magnitude of snow accumulation and melt, snowpack energy and mass fluxes may change in response to alterations in available energy. The snowpack energy balance is influenced by temperature and vapor density gradients within the snowpack and driven by energy exchange at the snow–atmosphere and snow–soil interfaces (Male and Granger, 1981). Future increases in mean air temperature and increased atmospheric longwave radiation emission will alter the snowpack energy balance (Franco et al., 2013), and the turbulent exchange of heat and moisture between the snowpack and the atmosphere. How these changes will impact energy partitioning, the snowpack mass balance, and water availability for ecosystem services and downstream users is largely unknown (Link and Marks, 1999). Modeling future snowpack conditions can be a useful technique for quantifying climate-related changes to hydrologic regimes in snowmelt-dominated ecosystems. Modeling studies have projected a wide range of potential future snowpack conditions by the end of the century with 5–60% decreases in SWE (Bavay et al., 2009; Beniston et al., 2003; Lopez-Moreno et al., 2009), 1–8 weeks earlier snowmelt (Bavay et al., 2009; Beniston et al., 2003; Gillan et al., 2010; Stewart et al., 2004), and an overall shorter snow season (Lopez-Moreno et al., 2009; Magnusson et al., 2010). However, modeling studies are rarely, if ever, evaluated relative to experimental climate manipulations intended to alter dynamics of snow accumulation and melt.

This study uses IR heaters in the subalpine forest of Niwot Ridge, CO to explore the sensitivity of snow accumulation, snowmelt, and soil microclimate to IR heating. Comparisons to measurements made in control plots and to a naturally warmer subalpine snowpack in New Mexico were used to assess the validity of the IR heater manipulations with respect to snowpack conditions. Observed meteorological conditions and a physically based snowmelt model were used to estimate snow–atmosphere energy exchanges, and to identify mechanisms likely controlling observed changes in snow and soil properties. The driving question behind this research is: How do IR heaters affect snow accumulation, snowmelt, soil microclimate, and the partitioning of available energy at the snow–atmosphere interface?

2. Study areas

2.1. Niwot Ridge, Colorado

Niwot Ridge is located in the Colorado Front Range 35 km west of Boulder, CO and ~8 km east of the Continental Divide (40° 03′ N, 105° 36′ W) (Fig. 1). This area is designated a UNESCO Biosphere Reserve and is the location of the National Science Foundation (NSF) Niwot Ridge Long-Term Ecological Research (NWT LTER) site. The IR heating experiment is at 3060 m in subalpine forest composed of lodgepole pine (*Pinus contorta*), Engelmann spruce (*Picea engelmannii*), subalpine fir (*Abies lasiocarpa*), and limber pine (*Pinus flexilis*). Average canopy height at the nearby Ameriflux site is 11.4 m with an average gap fraction of 17% (Turnipseed et al., 2003). Maximum LAI during the growing season is 4.2 m^2 m^{-2}. The secondary forest around the study site is approximately 100 years old following major logging activity in the earlier part of the 20th century. Prevailing wind direction is from the west, especially during winter,

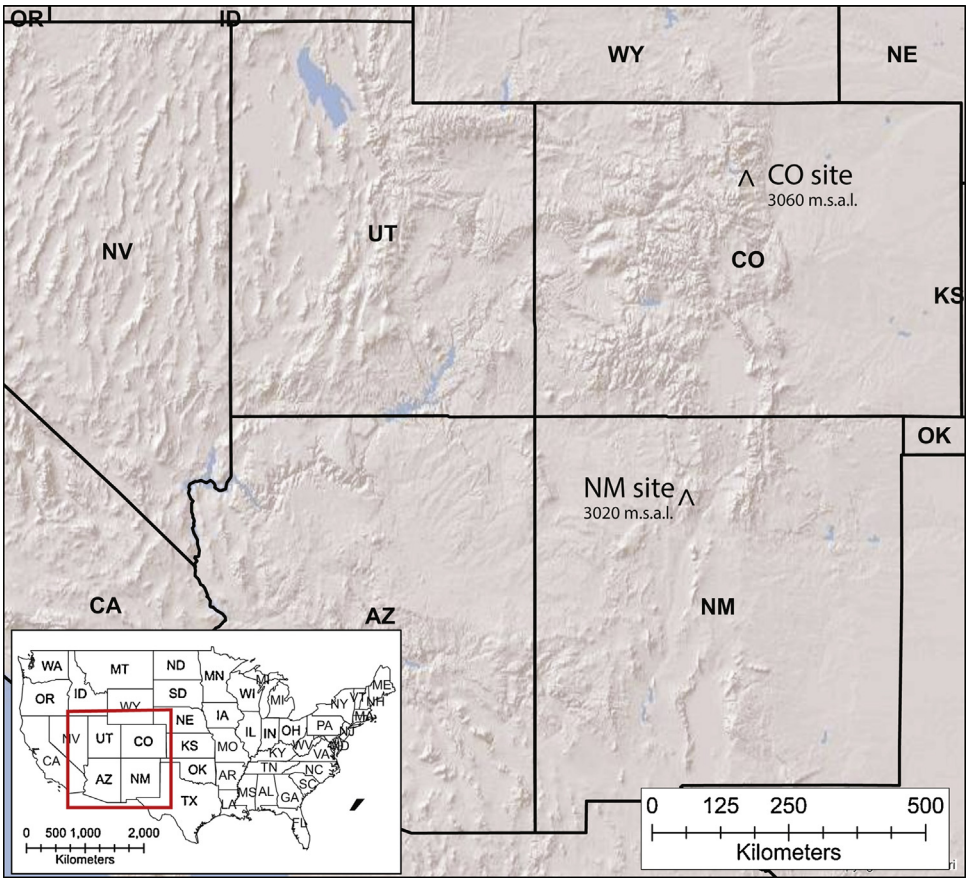

Fig. 1. Niwot Ridge, CO and Valles Caldera National Preserve, NM site locations.

with low sub-canopy windspeeds (Blanken et al., 2009; Turnipseed et al., 2003). Average winter-time relative humidity during the study period was 57%. The surface surrounding the study site is generally flat with a slope of <5% in each study plot. The soils are rocky, having developed on igneous and metamorphic residuum or till, and are classified as loamy-skeletal, mixed, superactive Typic Dystrocryepts. The mineral soil is covered by a thin (~2 cm) organic layer which may reach up to 15 cm in depth (Castanha et al., 2013).

Long-term meteorological, snowpack, and flux measurements are made at the nearby C-1 site, the National Resources Conservation Service SNOwpack TELemetry (SNOTEL) network site NIWOT 663, and at a flux tower site, all of which are located within 0.5 km from the experiment site. The long-term (1952-present) mean annual air temperature is 1.5 °C. Niwot Ridge experiences an average of 930 mm annual precipitation, about 80% of which falls as snow (Caine, 1995). Snowpit measurements are made as part of the Niwot Ridge Long Term Ecological Research program, including vertical profiles of snowpack density and snow temperature.

2.2. Valles Caldera National Preserve, New Mexico

The Valles Caldera National Preserve (VCNP) Mixed-Conifer site is located in the Jemez Mountains of northern New Mexico (NM) (35° 53′ 18″ N; 106° 31′ 36″ W) at 3020 m elevation (Fig. 1). The vegetation at this study site is mainly composed of Douglas fir (*Pseudotsuga menziesii*), white fir (*Abies concolor*), blue spruce (*Picea pungens*), southwestern white pine (*Pinus strobiformis*), limber pine (*Pinus flexilis*), ponderosa pine (*Pinus ponderosa*), and some aspen (*Populus tremuloides*). Average canopy height around the flux tower is 19.6 m, and growing season LAI is 3.43 m^2 m^{-2} (McDowell et al., 2008). Soil texture at this site is a sandy loam, roughly 150 cm deep overlying volcanic parent material (Small and McConnell, 2008). Average annual precipitation is 720 mm. Supplementary precipitation data were collected 14 km away at the Quemazon SNOTEL site at an elevation of 2896 m. Approximately 65% of the precipitation in the Jemez mountains falls as snow between November and April and 35% falls as rain associated with the summer monsoon. Average wintertime relative humidity during the study period was 55%.

3. Field methods

3.1. Experiment design

The CO study site has 20 circular plots, 3 m in diameter (7.07 m^2), 10 of which are heated and 10 of which are controls (Fig. 2a). Heated plots are surrounded by a hexagonal steel structure with six infrared lamps arranged evenly around the plot perimeters. The heaters were mounted 1.2 m above bare ground (Fig. 2b), and the heating lamps were angled at 45° to evenly distribute the radiation across the plot area (Kimball, 2005; Kimball et al., 2008). Unlike other snow manipulation methods, this design does not interfere with wind, sunlight, or precipitation, nor does it physically disrupt the snowpack.

The ceramic IR lamps (Mor Electric Heating Association Inc. Model FTE-1000) were 245 mm long by 60 mm wide with a maximum output of 1000 W. The energy emanating from heaters was in the thermal infrared portion of the electromagnetic spectrum at 4.5–42 μm, consistent with previous warming experiments (Kimball, 2005; Wan et al., 2002). From a surface energy balance perspective, the energy from the heaters was equivalent to an increase in incoming longwave radiation to the snow surface. Heater output was designed to increase surface soil temperature

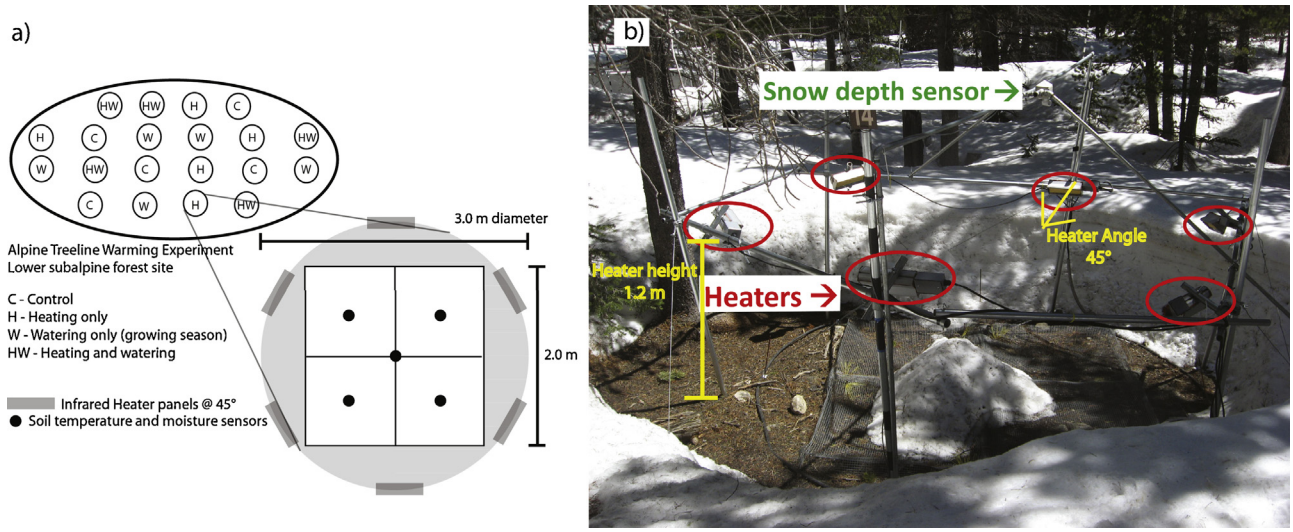

Fig. 2. Schematic showing layout of heated and control sites (a). Photo of example heated plot taken on 31 May, 2011 (b), heaters are circled in red at the vertices of the heated structure hexagon. Note in (a) that each plot was divided into quadrants with soil moisture and temperature measured at the center of each quadrant within each plot. Watered plots (W) and heated and watered plots (HW) were not used in this study. (For interpretation of the references to color in this figure legend, the reader is referred to the web version of the article.)

by ~4–4.5 °C averaged over the growing season, a mid-range temperature increase projected for the end of the century (IPCC, 2007); heaters were operated in a constant flux mode (Harte and Shaw, 1995; Harte et al., 1995). In 2009–2010, heater output was maintained at the same level year round. In subsequent years it was moderated with the aim of advancing the date of snow disappearance by ~4 weeks.

We explored snowpack sensitivity to different energy inputs by comparing results from years (water years 2010–2012) with different IR heater energy outputs. During water year 2010 season, heaters operated at 50% power or ~500 W. In very low wind conditions, we estimated that ~50% of heater output was incident within the plot perimeter (Kimball, 2005), resulting in an estimated radiant flux density of ~214 W m^{-2}. During the 2010–2011 winter season (mid-November through mid-March), heater output was lowered to 10% of maximum power resulting in a radiant flux density of 42 W m^{-2} in each heated plot. In mid-March, heaters were turned up to 20% resulting in a radiant flux density of 85 W m^{-2} at each heated plot in order to achieve an advance in the timing of snowmelt. For the 2011–2012 winter season, the heaters operated at 10% of maximum output (42 W m^{-2}) from mid-November through the first week in March. From then onward, heaters operated at 40% of maximum power (171 W m^{-2}).

3.2. Meteorological measurements

Meteorological measurements at the CO site were recorded from a tower located in the center of the study site including an RM Young Model 03101-L anemometer measuring wind speed, and a Campbell Scientific HMP45C-L Temperature/Humidity Probe (Table 1). All meteorological sensors were mounted 2 meters above bare ground, and data were logged as 15 min averages of 1-s readings. Additionally, above-canopy radiation (25.5 m), temperature and wind speed measurements (both 21.5 m) were obtained from the Niwot Ridge AmeriFlux tower (Table 1), located 0.5 km from the study site. For the few existing data gaps, an average value from the preceding and subsequent timestep was used to fill the gap. Meteorological and radiation measurements for the New Mexico site were collected from a flux tower as described in Molotch et al. (2009). The specific instruments are listed in Table 1.

3.3. Snow measurements

Snow depth measurements over selected heated and control plots at the CO site were recorded using Judd Communications LLC Ultrasonic snow depth sensors. These sensors became operational on 5 March 2010, on 29 January 2011, and on 3 November 2011 in each respective winter. Each snow depth sensor was 8 cm × 8 cm × 13 cm in size with a beamwidth of 22° and a vertical accuracy of 1 cm. Depth was recorded hourly with a Campbell Scientific CR1000 datalogger. Each snow depth sensor was located about 2 m above bare ground.

For the 2009–2010 snow season, four pairs of heated and control plots were set up at the study site. The 2010–2011 snow season had only two heated and control pairings due to field equipment and electrical malfunctions. Three heated and control pairs operated throughout the 2011–2012 season. Snow depth in each plot was also measured by hand every two weeks from November until the end of each snow season (i.e. the date of snow disappearance).

The New Mexico snow measurements for the 2009–2010 snow season were recorded with nine Judd ultrasonic snow depth sensors in the vicinity of the flux tower. The sensors were positioned in a stratified sampling pattern regarding proximity to trees with three sensors in under-canopy locations, three at canopy-edge locations, and three in open areas (Molotch et al., 2009). Since the above-mentioned snow sensors were not operational in the following two snow seasons (2010–2011 and 2011–2012), snow depth and SWE in 2011 and 2012 were measured at a COSMOS (Cosmic Ray Soil Moisture Observing System; http://cosmos.hwr.arizona.edu/) site approximately 300 m from the flux tower (Desilets et al., 2010).

3.4. Soil measurements

Inside the heated and control plots, soil volumetric water content (VWC) and soil temperature were measured with Decagon EC-TM sensors at 5–10 cm soil depth. Sensors were inserted vertically into the soil at the center of four 1 by 1 m quadrants within the plot. Soil probes were calibrated in the laboratory to VWC ranging from dry to saturated using soil collected adjacent to plots and sieved to remove particles >2 mm (Moyes et al., 2013). Data were recorded every 15 min with averages of the four sensors in each plot used to calculate average VWC and soil temperature per plot.

Table 1
Instrument descriptions and measurement heights on Niwot Ridge, CO and in the Valles Caldera, NM.

Variable	Niwot Ridge, Colorado		Valles Caldera, New Mexico	
	Measurement height (m)	Instrument	Measurement height (m)	Instrument
Temperature (°C)	2 & 21.5	Vaisala HMP-45C & Vaisala HMP-35D	21.65	CSAT-3 Campbell Scientific
Relative humidity (%)	2 & 21.5	Vaisala HMP-45C & Vaisala HMP-35D	21.65	Vaisala HMP-45C
Wind speed ($m\,s^{-1}$)	2 & 21.5	RM Young 03101-L & CSAT-3 Campbell Scientific	21.65	CSAT-3 Campbell Scientific
Net radiation (W/m^2)	25.5	CNR-1, Kipp & Zonen	20	4-component CNR-1, Kipp & Zonen
Heaters	1.2	Mor Electric Heating Association, Inc. ceramic heaters FTE-1000	N/A	N/A
Snow depth (cm)	1.75–2	Judd Comm. Ultrasonic Snow Depth Sensors	2.5	Judd Comm. Ultrasonic Snow Depth Sensors
Soil temperature (°C)	−0.1 to −0.05	Decagon EC-TM	−0.4 to −0.01	CS 107 Thermistors
Soil moisture (% by volume)	−0.1 to −0.05	Decagon EC-TM	−0.4 to −0.1	CSI CS616 TDR probe
Precipitation	Sub-canopy	100″ Transducer, Sensotec (@SNOTEL)	2	TE525WS-L, Texas Electronics

At the NM site, hourly soil microclimate data were collected from the Western Regional Climate Center's (WRCC) Redondo site. This soil and meteorological instrument cluster is located 1.7 km west of the VCNP Mixed-Conifer study site where the flux tower and snow measurements were located. Here, VWC was measured with Campbell Scientific CS616 Time Domain Reflectometry (TDR) probes with an integrated depth of 1–40 cm, and soil temperature was measured with CS 107 Thermistors at depths of 1, 10, and 40 cm.

4. Modeling methods

SNOWPACK, a complex, one-dimensional physical snowpack model (Bartelt and Lehning, 2002; Lehning et al., 2002a,b), was used to model snowpack mass and energy fluxes at the control, heated, and NM sites. SNOWPACK numerically solves the partial differential equations governing mass, energy, and momentum conservation within the snowpack using a fully implicit Lagrangian Gauss-Seidel finite element method. Snow is modeled as a three-component porous structure comprising volumetric fractions of solid and liquid water, and air. Snowpack behavior is characterized by two mass conservation equations for the different phases of water, one bulk temperature equation and one momentum equation for the ice phase (Bartelt and Lehning, 2002). Rates of snowpack settlement and explicit properties of multiple layers are calculated based on a microstructure-dependent viscosity determined by the temperature and temperature gradient of the snowpack (Lehning et al., 2002b). SNOWPACK outputs utilized in this study include snow depth, snow water equivalent, snow grain size, snow temperature, and energy fluxes at the snow–atmosphere interface; other outputs include snow grain morphology, snow density.

4.1. Model forcings

SNOWPACK is forced by air temperature, relative humidity, wind speed, snow–soil interface temperature, incoming shortwave and longwave radiation, precipitation and/or snow depth. Geographic locational information, vegetation density, and soil properties are static model parameters. The instruments, locations, and measurement heights for each variable are described in Table 1. It should be noted that precipitation data from the Niwot SNOTEL site was scaled by a factor of 0.9 in 2010 and 0.8 in 2011 to correct for slight precipitation gauge over-catch during the snow season. This was based on the measured ratio of precipitation and SWE during discrete snow events as determined from the gauge-measured liquid depth of precipitation and SNOTEL snow pillow SWE measurements (under the assumption that the snow pillow has greater accuracy). No correction was necessary for 2012 precipitation data based on comparisons with the snow pillow. The Beer's Law extinction coefficient default value of 0.7 in SNOWPACK was changed to 0.4 to reflect the local canopy conditions. Because future changes in precipitation are predicted with far less certainty than projected temperature changes (Stocker et al., 2013), no precipitation changes were accounted for in this study. Previous studies have reported snowfall over-catch (Li and Pomeroy, 1997; Struzer, 1971; UNESCO, 1978; Benning and Yang, 2005; Williams et al., 1998a,b; Yang et al., 2000; Yang and Ohata, 2001) and have used measured SWE to infer precipitation gauge efficiency (e.g. Yang et al., 2000; Goodison, 1981; Goodison et al., 1998). Our correction uses snow pillow SWE data surrounding the storm events when atmospheric humidity is high and temperature is low, limiting biases due to sublimation or melt. Bias from wind-scour in the forest clearing where measurements are made is also unlikely.

4.2. Modeling scenarios

4.2.1. Control simulations

Each model was run with hourly data; radiation data came from the flux tower at Niwot Ridge, precipitation and air temperature from the Niwot SNOTEL, and relative humidity and windspeed data were from the in situ instrumentation at the CO study site described above.

4.2.2. Heated simulations

Heated model runs in CO were performed by using the same driving data as for control simulations, but increasing the amount of measured incoming longwave radiation (LW_{in}) by the amount added to each plot from the heaters as previously described in Section 3.1.

4.2.3. New Mexico simulations

To evaluate whether IR heaters produce similar effects on snow as would warmer air (the primary mechanism of surface warming in the future) (Amthor et al., 2010), we also modeled snowpack at the naturally warmer NM site. The NM simulations were driven with meteorological data (air temperature, relative humidity, windspeed, precipitation, incoming solar and longwave

radiation) from the instruments at the Valles Caldera Mixed-Conifer flux tower site described above.

4.2.4. Synthetic warming simulations

Although the NM site has been shown to be a useful warming analog for the Colorado (CO) site (Molotch et al., 2009), there are climatological differences associated with latitude, humidity, and precipitation that can complicate comparisons with the CO site. To address some of these differences, synthetically warmed simulations at the CO site were also conducted using the CO control forcings, yet systematically increasing air temperature and incoming longwave radiation values based on observed monthly differences between the CO and NM sites. Unlike the NM simulations, this simulation includes precipitation forcings identical to the CO Control simulations. Adjusted incoming longwave radiation was derived based on estimates of effective atmospheric emissivity and synthetically warmed air temperature. Effective atmospheric emissivity (ε_a) was calculated from hourly measurements of LW_{in} and air temperature observed at the CO site:

$$\varepsilon_a = \frac{LW_{in}}{\sigma T^4} \quad (1)$$

where σ is the Stefan–Boltzmann constant ($5.67 \times 10^{-8}\,W\,m^{-2}\,K^{-4}$), and T is air temperature in Kelvin. With this calculated ε_a value, a new hourly LW_{in} time series was calculated by adding the average difference in temperature between NM and CO to the measured CO air temperature (T_{new}), and using the Stefan–Boltzmann Law:

$$LW_{new} = \varepsilon_a \sigma T_{ew}^4 \quad (2)$$

SNOWPACK model runs for each of the four cases–control, heated, synthetic, and NM – in 2010, 2011, and 2012 were produced for October–June. We compared snow depth, soil temperature and moisture, and energy fluxes over the entire snow season and separately for the accumulation and melt periods. The snow season is defined based on the duration of snow cover from first snowfall in autumn to snow disappearance in spring; each snow season is referred to as the year of snow disappearance (i.e. the 2010 snow season began in autumn of 2009). The accumulation season was defined to be the time from initial snow accumulation until snowmelt onset. The snowmelt period was defined as beginning at the onset of snowmelt until snow disappearance. The exception to these definitions is the heated case in 2010 due to its ephemeral nature, thus new definitions for this case were based on the largest individual accumulation and melt-out event from 7 May to 17 May. Snowpack accumulation and melt timing and magnitude as well as average energy and water fluxes for the "accumulation" period were calculated from 7 May to 12 May 2010 (accumulation event). Melt calculations were for average fluxes and mass losses or gains from 13 May through 17 May 2010.

Energy and mass fluxes are reported from the perspective of the snowpack, thus gains to the snowpack energy and mass are reported as positive, losses from the snowpack are reported as negative. The snowpack energy balance is generally expressed:

$$\Delta Q_S = QSW + QLW + Q_e + Q_h + Q_g + Q_A \quad (3)$$

where ΔQ_s is the change in energy storage associated with both cold content and snowmelt, QSW, QLW, Q_e, Q_h, Q_g, and Q_A are the net shortwave radiation, net longwave radiation, latent heat flux, sensible heat flux, ground heat flux at the snow–soil interface, and energy flux due to advection, respectively. Once the temperature of the snowpack reaches 0 °C, any additional energy input to the snowpack is converted to melt energy.

5. Field results

5.1. Meteorology

Mean air temperature at the Niwot Ridge SNOTEL site in CO was −0.79, 0.73, and 0.98 °C in 2009–2010, 2010–2011, and 2011–2012 snow seasons, respectively (Fig. 3). This site is sheltered with low daily wind speeds below the canopy averaging 0.43, 0.43, and 0.45 m s^{-1} in each of the three study years, respectively. During the 2009–2010 snow season, snow depth measurements at the Niwot SNOTEL site show snow accumulation beginning in early November 2009 and melting out completely by May 31. The 2010–2011 snow depth measurements show snow accumulation beginning in late October and melting out completely by June 10. The 2011–2012 snow depth measurements show snow accumulation beginning in mid-October and melting out completely by May 5.

Mean air temperature at the NM site was −0.69, 2.27, and 3.93 °C in 2009–2010, 2010–2011, and 2011–2012 snow seasons, respectively. Air temperature time series at the two sites track each other fairly well (Fig. 3) with average snow season air temperature at the Quemazon site consistently 3–4 °C higher than at the Niwot SNOTEL site. This indicates that the NM site adequately reflects a naturally warmer condition relative to the CO site. Average daily wind speeds above the canopy were 2.96, 1.81, and 1.34 m s^{-1} in each of the three study years (note: below-canopy windspeed measurements were not available). Snow accumulation in the Valles Caldera 2009–2010 season began in late November and melted completely by May 6. Snow accumulation in the 2010–2011 season began in mid-December and snow disappeared on May 2. Snow accumulation in the 2011–2012 season began in early November and snow disappeared by April 19.

5.2. Snow accumulation and melt

During the 2009–2010 snow season when heaters were set to 50%, average maximum snow depth in heated plots (31 cm) was 74% lower than the control plots (121 cm). Maximum snow depth at the NM site (99 cm) was 18% lower than the CO control plots. Thus, the heaters reduced snow accumulation far beyond that observed at the naturally warmer site (Figs. 4 and 5). In the heated plots, snow was present only directly after snow events, and melted quickly, never reaching depths greater than 31 cm. The ultrasonic snow depth sensors were able to capture this transient snow accumulation and melt in the heated plots. Snowmelt onset began 60 days earlier in NM relative to CO control snowpack, and disappeared 25 days earlier than the CO control plots. Melt onset and snow disappearance in the heated plots were not comparable to the control or NM snowpacks due to the transient nature of the snowpack.

During the 2010–2011 snow season, when heaters were set to 10–20%, average maximum snow depth was 116 cm in heated plots, 9% less than average maximum depth in control plots of 128 cm. These differences were relatively small during the snow accumulation period but became more pronounced during the snowmelt period. NM average maximum snow depth (58 cm) was 55% lower than CO control plots. Snowmelt onset and snow disappearance at control and heated plots occurred within 1 day of each other. Snowmelt onset occurred 72 days earlier in NM versus the CO control site, and snow disappeared 37 days earlier in NM.

During the 2011–2012 snow season, when heaters were set to 10–40%, average maximum snow depth was 92 cm in heated plots, 4% less than average maximum depth in control plots; differences in snow depth were particularly notable during spring. NM snow depth was 13% greater than average maximum depth in CO control plots with considerably greater snow depth in fall. Unlike previous years, snowmelt onset occurred earliest in control plots; 4 days earlier than heated plots and 17 days earlier than the NM site. Snow

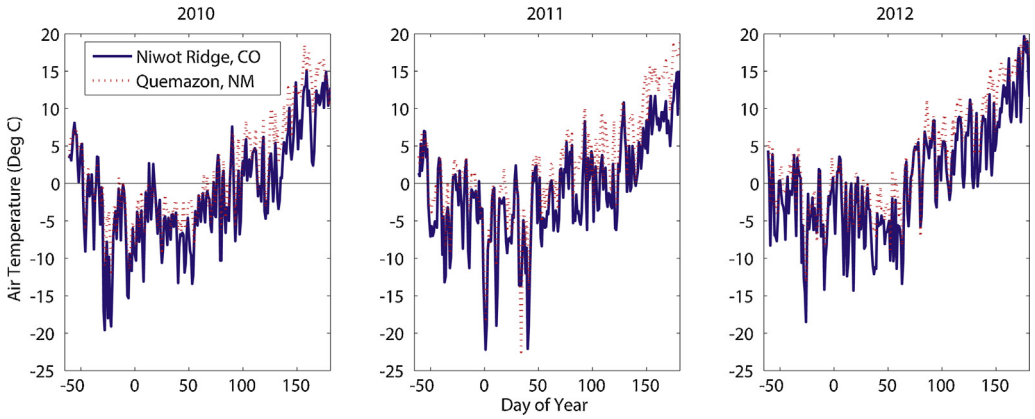

Fig. 3. Daily mean air temperatures at the Quemazon, NM and Niwot Ridge, CO SNOTEL sites for the 2010, 2011, and 2012 snow seasons.

disappeared 31 days earlier in heated plots and 6 days earlier in NM plots relative to controls. It should be noted here that, in all years, snow persisted in the center of these heated plots (Fig. 2b) days to weeks longer than the snow directly underneath the heaters, thus creating an annulus void shape with greater snow depths around the perimeter and at the center of the plot. Thus, the observed snow depths from the ultra-sonic sensors are likely greater than the plot-average snow depth.

Averaged over all study years, heated and NM snowpacks experienced 30% and 23% lower peak snow accumulation, respectively, compared to control plots; results were strongly influenced by the large snowpack reductions in the 2009–2010 snow season. Control plots experienced the greatest number of snowcover days (average 226); heated plots and NM had fewer days of snowcover with an average 155 and 149 days, respectively. These general data summaries indicate that the snowpack response to the heating manipulations fell within the range of the naturally warmer conditions in NM with the exception of the 2009–2010 snow season when the heaters were set relatively high.

5.3. Soil temperature

Average snow season soil temperature in CO control plots for all study years was 2.6 °C compared to 4.4 °C in heated plots and 4.2 °C in NM (Fig. 6). Pre-snowmelt average soil temperature in control plots was 0 °C compared to heated soil at 1 °C

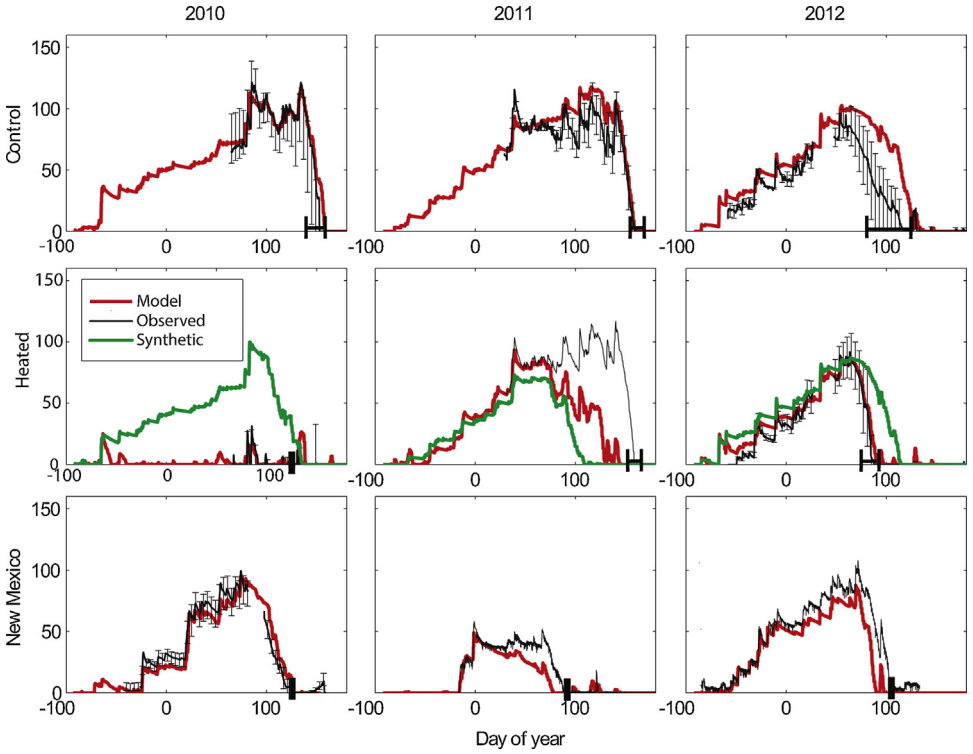

Fig. 4. Modeled and observed snow depth from ultra-sonic sensors for control, heated, synthetic, and New Mexico plots. Note the vertical bars bracketing observed values in all plots represent the range in the observations from all sample locations; heated 2011, NM 2011, and NM 2012 only have 1 observation each and thus a range is not shown. The black horizontal lines along the *x*-axes in control and heated graphs indicate the date range of observed snow disappearance determined from soil temperature measurements.

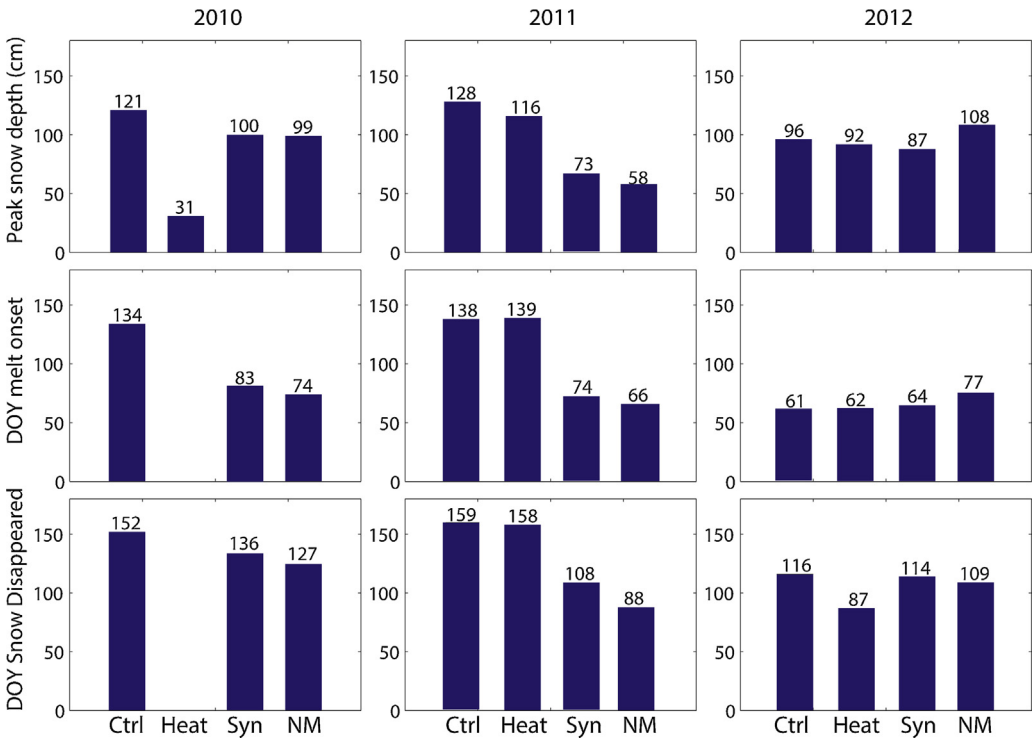

Fig. 5. Observed (modeled for synthetic) peak snow depth, and melt onset and snow disappearance timing for the control, heated, synthetic, and New Mexico plots 2010–2012. Note the day of year (DOY) of melt onset and snow disappearance are not shown for the heated plots in 2010 due to the intermittent snowpack.

which was mostly snow-free during the 2010 winter and thus warmed above freezing. NM pre-snowmelt soil temperatures averaged −0.14 °C. From snowmelt onset through the end of June, average soil temperatures in heated plots and NM (9.7 °C and 6.9 °C, respectively) were warmer than control plots (6.4 °C). In all years, the greatest differences between heated and control soil temperatures occurred at time periods when heated plots became snow free. In this regard, one can see large differences in soil temperatures throughout most of 2010 and during the spring of 2012. Conversely, in 2011 there was very little difference in soil temperature in heated and control plots because heaters were set lower and therefore snow persisted in heated plots.

5.4. Soil moisture

Average VWC in CO control plots for all study years was 0.20 over the entire snow season compared to 0.22 in heated plots and 0.20 in NM (Fig. 6). Pre-snowmelt average VWC in control plots was slightly lower than in heated plots at 0.18 versus 0.21, respectively. VWC was similar after snowmelt onset in control plots compared to heated plots, 0.24 versus 0.23. Average VWC in NM was similar to, or lower than control and heated plots, with pre-snowmelt and post-snowmelt onset VWC values of 0.18 and 0.21, respectively. As with soil temperature, the greatest differences in VWC are seen during periods when snowmelt occurs in heated plots but not in control plots; i.e. throughout 2010 and in spring of 2012.

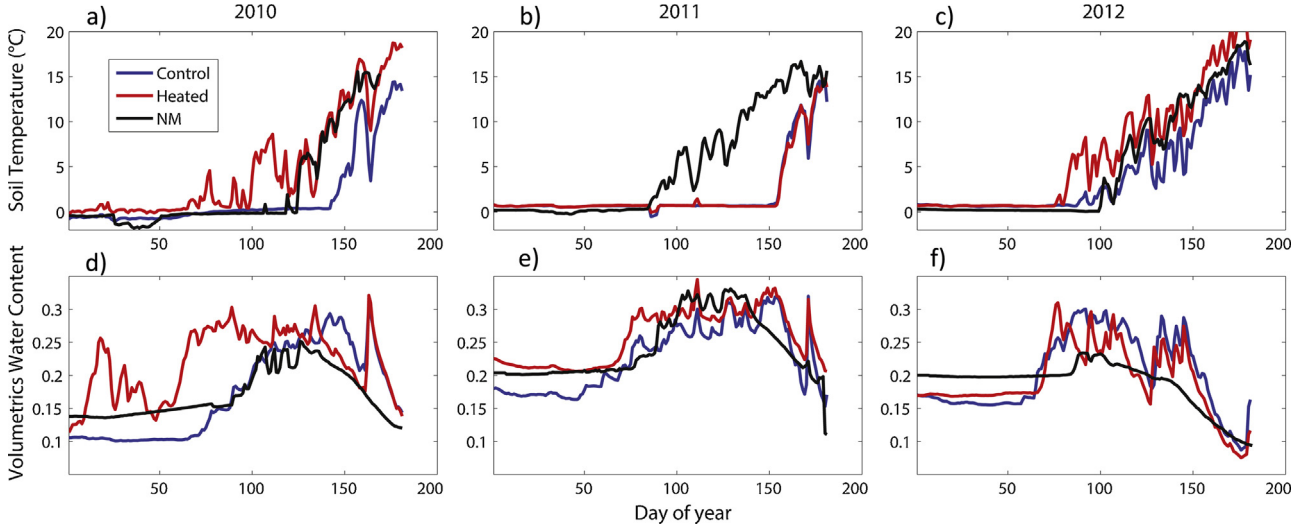

Fig. 6. Measured soil temperature (a–c) and soil moisture (d–f) for control, heated, and New Mexico study plots 2010–2012, respectively.

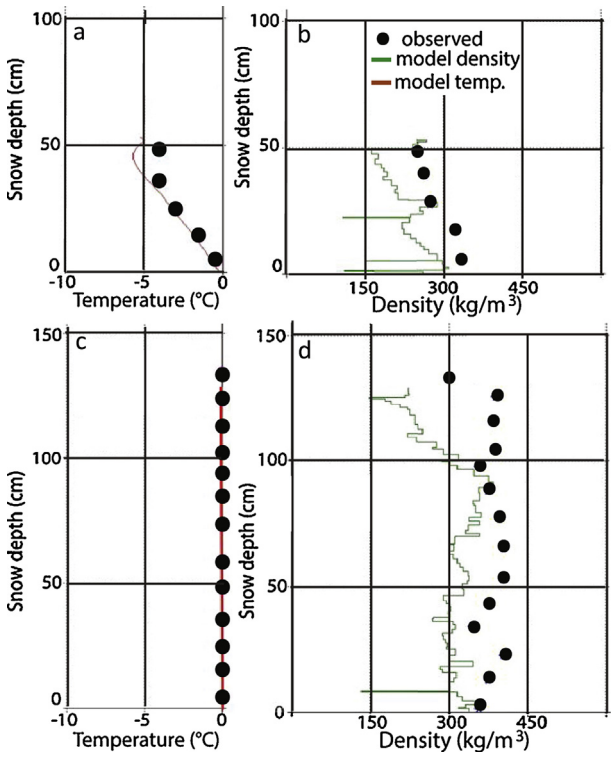

Fig. 7. Modeled and observed snowpack temperature and density profiles for 1/13/2010 (a and b) and 5/18/2011 (c and d). Observations were taken adjacent to the Colorado study plots near the Niwot Ridge C-1 climate station.

6. Model results

6.1. Model validation

Model estimates of snow accumulation and melt reflected observed values relatively well (Fig. 4). Model RMSE ranged from 6 to 15 cm in control plots, 3–30 cm in heated plots, and 6–12 cm at the NM site. SNOWPACK tended to underestimate peak depth by between 23 and 4 cm, except in the 2012 control case where peak snow depth was overestimated by 7 cm. Model errors showed little temporal variation for control simulations in 2010 and 2011 whereas in 2012 model over-estimates of snow depth were more pronounced in spring (Fig. 4). Heated simulations tracked snow accumulation quite well in all years but snow depth was underestimated in spring of 2011. NM simulations matched observations relatively well in all years/time periods with slight low biases in spring snow depth in 2011 and 2012.

Comparison of observed and modeled bulk snowpack properties such as snow temperature and snow density show relatively good agreement during the mid-winter period (mid-January 2010). Modeled snow temperature fell within ~1 °C of observations, though snow density was underestimated by 9–30% (Fig. 7). During the snowmelt season, both observed and modeled snow temperatures were 0 °C in the isothermal snowpack. The model underestimated snow density by between 4 and 25% in the bottom 100 cm, and by up to 60% in the top 40 cm of the snowpack.

6.2. Modeled snowpack conditions

Relative to control simulations, modeled snow depth at peak accumulation was 39% lower in heated simulations, 25% lower in synthetic simulations, and 31% lower in NM simulations. Modeled snow disappearance occurred 15–37 days earlier in heated plots, 2–51 days earlier in synthetic cases, and 30–82 days earlier in NM compared to control plots (Fig. 4). Consistent with observations, the heated snowpack in 2010 does not resemble any other cases, reflecting the ephemeral snowpack observed that year due to the higher heater output (Fig. 4).

Differences in modeled SWE between control and heated simulations were quite variable for the three years (Fig. 8). Similar to snow depth simulations, 2010 SWE simulations in heated plots exhibited significant intermittency with SWE values never exceeding 5 cm. Conversely, peak SWE in the control plots exceeded 30 cm. Synthetic and NM simulations exhibited remarkable similarities in terms of the timing and magnitude of peak SWE (i.e. 23 and 24 cm, respectively); 29% lower than control peak SWE. In 2011, peak SWE in the heated and synthetic simulations were 43% lower than control SWE. Differences between control and heated SWE were relatively small (<3 cm) during the accumulation period but were quite large during the snowmelt period (>10 cm). Peak SWE for the NM simulation was 74% lower than the control simulation; likely a result of the lower precipitation in 2011 at the NM site. In 2012, peak SWE for the heated simulation was 24% lower than the control simulation. SWE differences between control and heated simulations were slightly greater during the snowmelt period but, in general, were relatively consistent throughout the year when compared to the SWE differences simulated in 2011. Synthetic SWE simulations tracked the control simulations throughout the accumulation season and had a peak SWE value only 1 cm less than control simulations. During the snowmelt period, synthetic simulations began to deviate from control simulations more dramatically with snow disappearance occurring 12 days earlier. The NM simulation closely tracked the heated simulation but had greater early season snowfall. It is important to note that these simulations have inherent uncertainties and therefore modeled SWE differences deviate from the observed snow depth differences shown in Figs. 4 and 5.

Pronounced differences in the vertical-mean snow grain size were simulated under the different scenarios (Fig. 9). In 2010, the intermittent nature of the heated simulation is evident in the grain size estimates whereby grain size increases throughout each melt event until snow disappeared (Fig. 9-top; vertical red lines). Conversely, control simulations show large grain sizes in fall; a condition that is typical in cold continental climates where large facetted crystals are common due to large vapor gradients within the snowpack. Control grain sizes show modest increases throughout the winter followed by more pronounced grain size increases during the snowmelt period. Synthetic simulations show similar grain size behavior as control simulations with greater grain growth rates during the snowmelt period owing to the greater simulated energy inputs to the snowpack. NM simulations show a general pattern similar to control and synthetic simulations with more variability throughout the winter. This likely resulted from the warmer winter temperatures and shallower snow depths at the NM site; with shallower snow depths the mean vertical grain size is more sensitive to new snowfall events. In 2011, snow grain size for control and heated simulations exhibited more similarity in general behavior due to the lower heater output versus 2010. Relatively large grain diameters (~2 mm) were simulated in fall for both heated and control simulations. During the winter period grain size was approximately 10% smaller for the heated simulation, likely due to a decreased temperature and vapor gradient in the snowpack and reduced faceted crystal growth. The earlier onset of snowmelt in the heated simulation is evident with greater grain growth rates in heated versus control simulations during the spring transition. Synthetic grain sizes exhibited similar behavior as the control simulations during the winter period but during spring, the rates of grain growth were more similar to the heated simulation. NM grain sizes in 2011 exhibited unique behavior relative to the

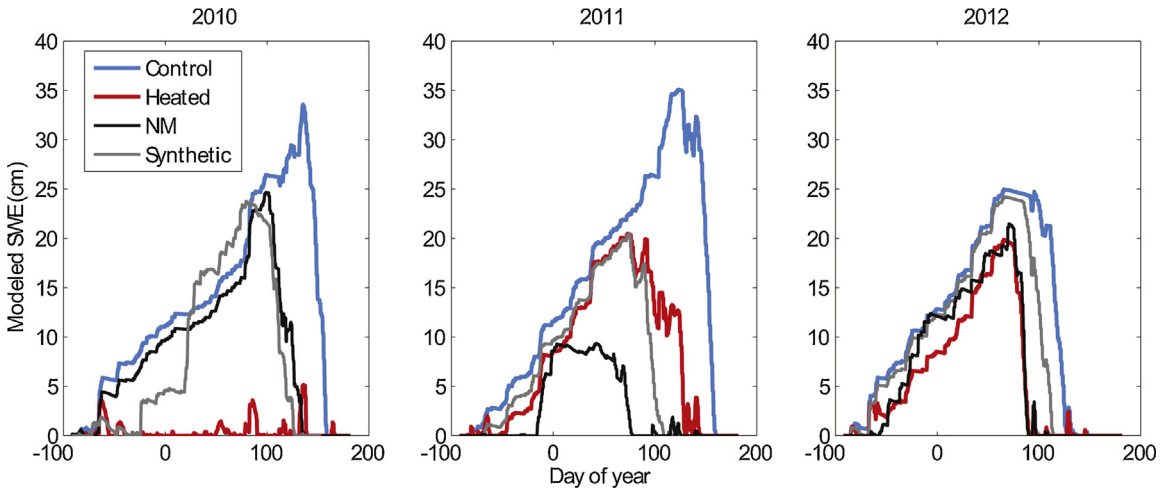

Fig. 8. Modeled SWE for control, heated, New Mexico, and synthetic warming scenarios for water years 2010–2012.

other scenarios because snow accumulation did not begin until winter. Grain size increased throughout the winter period up until the time of initial snow disappearance in early spring; intermittent snow accumulation and melt events can be seen during the spring period (vertical black lines). In 2012, heated simulation grain size was notably larger than the control simulation in fall. During the winter period all grain sizes were quite similar and in spring the heated simulation exhibited an earlier spring transition and associated earlier increases in grain size. The synthetic simulation grain size estimates largely tracked the control simulation and the NM simulation grain size values exhibited gradual increases throughout the simulation period which is consistent with the gradual increase in snow depth (Fig. 4).

Time series of vertical-mean modeled snow temperatures are shown in Fig. 10. Comparisons between control and heated

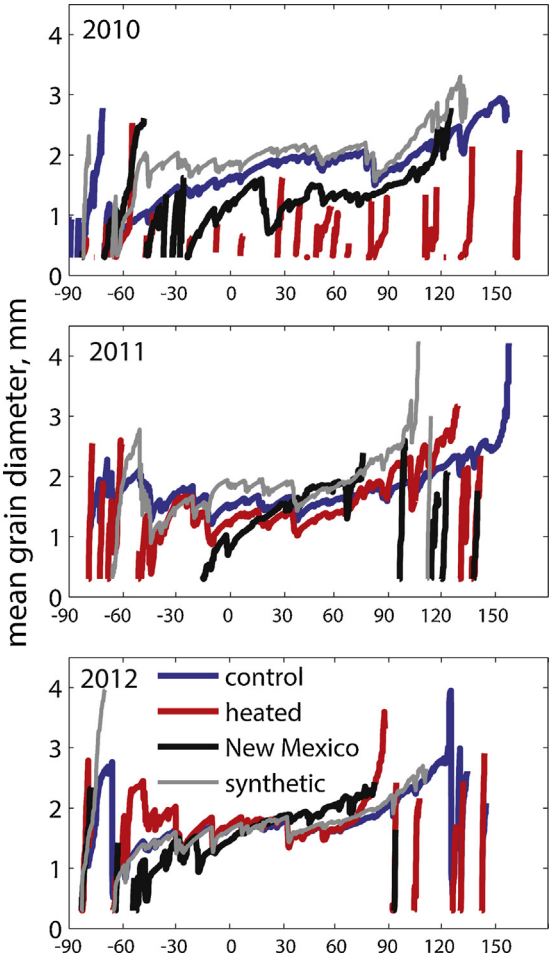

Fig. 9. Modeled vertically averaged snow grain size for control, heated, New Mexico, and synthetic warming scenarios for water years 2010–2012. (For interpretation of the references to color in text near the reference citation, the reader is referred to the web version of this article.)

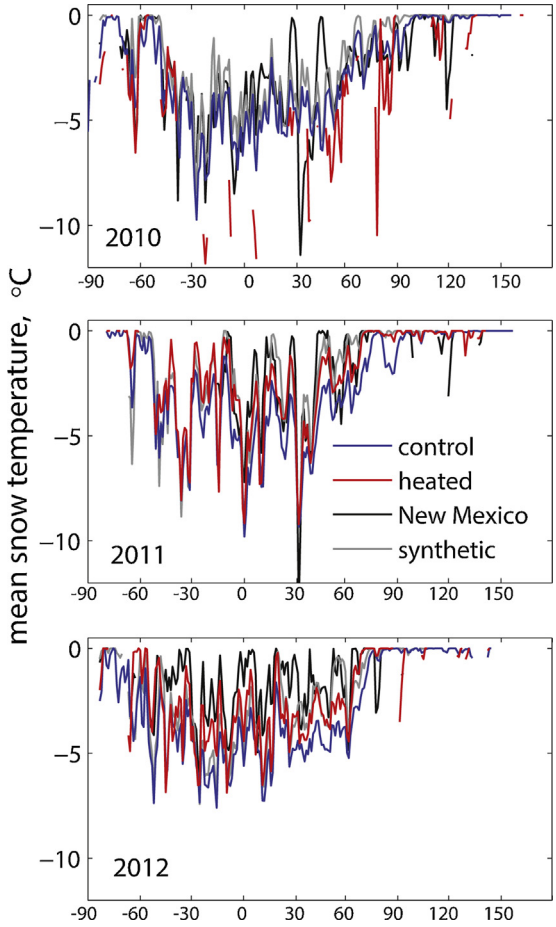

Fig. 10. Modeled vertically averaged snow temperature for control, heated, New Mexico, and synthetic warming scenarios for water years 2010–2012.

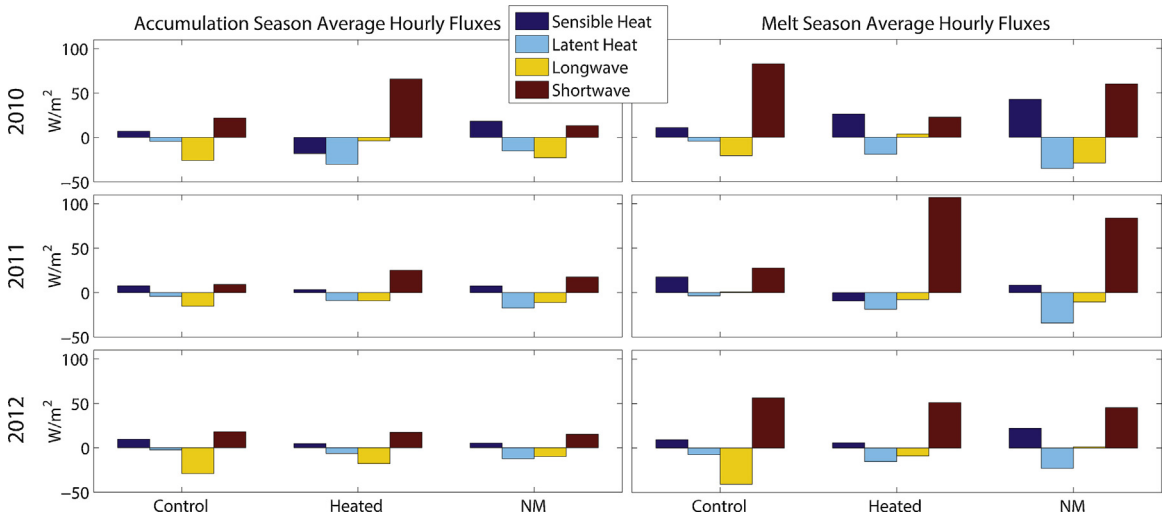

Fig. 11. Hourly average sensible, latent, net longwave radiation, and net shortwave radiation fluxes during the accumulation (left panels) and melt periods (right panels) modeled using SNOWPACK for the 2010–2012 snow seasons (top to bottom, respectively).

simulations are not particularly instructive in 2010 due to the intermittent nature of the snowpack in the heated simulation. In 2011 and 2012, a notable increase in snow temperature was simulated in heated plots relative to control plots with pronounced differences simulated during late winter and spring. During the winter period, NM and synthetic simulations had warmer snow temperatures than the heated simulations for both years but differences decreased in late winter/early spring. These snow temperature estimates are largely consistent with the grain size values shown in Fig. 9 in that colder snow temperatures are associated with larger grain sizes in fall (i.e. associated with facetted crystal growth) whereas warmer temperatures are associated with larger grain sizes in spring (associated with enhanced sintering and wet snow metamorphism). A detailed description of the physics linking snow temperature and snow grain size is beyond the scope of this paper and hence the reader is referred to McClung and Schaerer (2006).

6.3. Energy fluxes

The partitioning of individual components of the net radiative flux, net shortwave radiation (SW) and net longwave radiation (LW), differed between the control case and the warmer cases (Fig. 11). Net SW radiation was always an energy source to the snowpack while net LW radiation was usually an energy loss from the snowpack or zero (except the heated 2010 case). During the accumulation season net shortwave radiation was, on average, 86% greater in heated versus control simulations. Differences in net shortwave radiation in heated versus control simulations were variable, with an increase of 175% in 2011 versus a decrease of 3% in 2012; note 2010 values are not included in the average because a distinct snow accumulation period is not decipherable because of the intermittent snowpack. Accumulation season net longwave radiation increased by 39% on average in heated versus control plots with increases ranging from 40% in 2011 to 38% in 2012.

During the snowmelt period, net shortwave radiation in heated versus control simulations were 288% greater in 2011 and 9% lower in 2012. The differential net shortwave response to heating may be due to several factors which are revisited in Section 7. Net longwave radiation in heated versus control simulations were 11 times lower in 2011 and 78% greater in 2012. These large percentage differences should be viewed with caution as the magnitude of these fluxes are relatively small (Fig. 11); average net longwave radiation in heated versus control simulations in 2011 were $-7.9\,\mathrm{w\,m^{-2}}$ and $0.72\,\mathrm{w\,m^{-2}}$.

In general during both accumulation and melt seasons, a higher proportion of the total energy (sum of the absolute value of the fluxes) was partitioned into latent heat versus sensible heat in heated and NM simulations. During the accumulation season on average, modeled latent (Q_e) and sensible heat fluxes (Q_h) in control plots accounted for 7 and 15% of total energy exchange, respectively, while for synthetic simulations these fluxes accounted for 6 and 15% of total energy exchange on average, respectively (Fig. 11, Table 2). Conversely, energy partitioning for heated simulations was skewed toward Q_e versus Q_h, accounting for 18 and 10% of total energy exchange, respectively. Q_h was an energy source to the snowpack (positive) for all simulations except the 2010 heated case, a possible artifact of the heaters. This switch in energy partitioning toward more Q_e under warmer conditions is corroborated by the NM simulations where Q_e accounted for a greater percentage of total energy exchange than Q_h (26% versus 16%, respectively). Bowen (β) ratio (i.e. Q_h/Q_e) values indicate greater partitioning of available energy to Q_e rather than Q_h in heated and NM cases compared to control and synthetic cases (average β values of 0.32 and 0.69 versus 1.68 and 2.45, respectively).

Energy exchange during the snowmelt season for the control simulations was partitioned more into Q_h (16% of total energy exchange) versus Q_e (5%) on average (Fig. 11, Table 2). For synthetic simulations, melt-season Q_e accounted for 8% of energy exchange on average, and Q_h accounted for 7% on average. For heated simulations, melt-season Q_e accounted for 18% of energy exchange on average, and Q_h accounted for 16% on average. NM simulations exhibited the greatest proportion and magnitude of melt-season Q_e; 3–9 times greater than the control simulation magnitude. The heated simulations showed a Q_e flux that was 2–5 times greater than control (Fig. 11). Calculated β values during the snowmelt season further reveal the increased partitioning of available energy into Q_e in heated, NM, and synthetic simulations compared to the control simulations (i.e. average β values of 0.89, 1.06, and 0.88 versus 3.25, respectively).

6.4. Sublimation

Averaged for all years, heated and NM simulations show the greatest sublimation rates during mid-winter ($0.20–0.61\,\mathrm{mm\,d^{-1}}$), while control and synthetic simulations had lower sublimation

Table 2
Modeled sublimation and evaporation rates, modeled latent and sensible heat fluxes as proportions of total energy exchange during accumulation and melt periods.

	Accumulation				Melt			
	Control	Heated	Synthetic	NM	Control	Heated	Synthetic	NM
Mass loss (mm d^{-1})								
2010	−0.14	−0.61	−0.13	−0.45	−0.14	−0.72	−0.20	−1.11
2011	−0.11	−0.29	−0.12	−0.56	−0.45	−0.53	−0.49	−0.71
2012	−0.08	−0.20	−0.09	−0.40	−0.26	−0.53	−0.22	−0.80
Latent heat (%)								
2010	6.9	23.5	6.3	20.2	2.8	26.7	5.5	18.8
2011	10.8	18.5	6.2	30.5	6.8	9.1	10.6	19.6
2012	3.8	13.2	4.5	27.5	6.5	18.3	5.6	22.3
Sensible heat (%)								
2010	11.3	14.0	15.0	24.4	6.9	36.6	6.5	22.8
2011	19.8	6.9	13.7	13.1	32.5	4.6	3.7	4.8
2012	15.4	9.6	14.7	11.8	8.1	7.2	9.7	21.5

rates (0.08–0.14 mm d^{-1}) (Table 2). Vapor loss rates during snowmelt were also greatest for NM and heated simulations (0.53–1.11 mm d^{-1}), with NM rates 48% greater than heated plots on average. Sublimation rates were lower for control and synthetic simulations and ranged from 0.14 to 0.49 mm d^{-1} during the snowmelt period; on average 57% lower than average heated and NM sublimation rates.

As a percentage of total precipitation, sublimation amounts varied considerably for the different model scenarios. In 2010, the high heater output resulted in 100% of precipitation being partitioned to sublimation. Conversely, the control simulation in 2010 partitioned 11% of precipitation to sublimation. In 2011, sublimation percentages for control versus heated plots were more realistic at 7 and 14%, respectively and in 2012 they were 10 and 25%, respectively. The increased sublimation in the heated plots in 2011 and 2012 seem reasonable when compared against NM simulations (40 and 23%, respectively) but were larger than the synthetic simulations (3 and 6%, respectively).

7. Discussion

A consistent difference between the heated and control plots in CO and between NM and CO sites was the overall decrease in snow depth and SWE under warmer conditions. Previous studies have predicted SWE reductions of 35–60% in the coming decades (Adam et al., 2009; Beniston et al., 2003; Lapp et al., 2005; Lopez-Moreno et al., 2008), which are consistent with results from this study: average snow depth decrease of 56% in heated versus control plots. Previous works have observed a shift toward earlier snowmelt timing by 2–3 weeks (Clow, 2010; Hamlet et al., 2007) and melt is estimated to continue shifting earlier by 1–2 months in the future (Adam et al., 2009; Rauscher et al., 2008; Stewart et al., 2004). The predicted earlier snowmelt in these studies is comparable to the difference between control and heated snowpack melt timing; between zero and 5 weeks earlier snow disappearance. While the heated simulation results for 2010 are certainly outside the bounds of expectations, the results for 2011 and 2012 are consistent with previous works in similar climates (Molotch et al., 2007; Schulz and de Jong, 2004; Essery et al., 2003). Hence, as intended, the IR heaters generally produced changes to snow accumulation and melt timing consistent with expectations and previous model scenarios of climate warming.

Soil microclimate dynamics in snowmelt-dominated ecosystems are largely governed by snow depth and snowmelt timing (Filippa et al., 2009; Harte et al., 1995; Walker et al., 1999). Considering the soil temperature differences in the CO control plots compared to the naturally (NM) and experimentally (CO heated) warmer plots, the prediction of "colder soils in a warmer world" by Groffman et al. (2001) is contradicted by our results. Conversely, average soil temperature in NM before snowmelt onset was lower than both CO heated and control soil temperatures, suggesting that the heating experiment may not provide realistic projections of winter soil temperature beneath the snowpack. Given that IR heating experiments have the explicit goal of increasing soil temperature by a predetermined amount, they may not replicate hydrological and biogeochemical responses to warming. The New Mexico comparison illustrates that soils are colder in locations with shallower snow despite warmer air temperatures. As a result, the potential for soil freezing and reduced infiltration rates may be considerable. The colder soils would also reduce microbial activity during the winter season and therefore decrease soil respiration (Monson et al., 2006). These processes would not be replicated using IR heaters given the method of energy application to the surface.

Trends in soil moisture, evapotranspiration (ET), and runoff in snowmelt-dominated basins of the western US are highly correlated to shifts in snowmelt timing (Hamlet et al., 2007) with model predictions (Vicuna et al., 2011) and observations (Molotch et al., 2009) suggesting that earlier snowmelt leads to enhanced water losses via ET. Our results show snow disappearance in heated plots 1–4 weeks earlier than control plots. These results are significant in that earlier snowmelt increases soil moisture in early spring but may result in reduced soil moisture in late spring/summer. While these changes are somewhat intuitive, the increased soil moisture observed here is counter to previous IR heating experiments in rain-dominated climates (Wu et al., 2011). The differential response of soil moisture to warming in the presence of snow occurs because water inputs to the system are dependent on energy available for snowmelt. As a result, increased energy inputs result in snowmelt and associated increases in soil moisture. Conversely, in rain-dominated systems, increases in energy availability at the surface drives greater evaporation and associated decreases in soil moisture. Given that photosynthetically active radiation is relatively high in summer, the shift in the timing of soil water availability may result in a decrease in ET and reduced vegetation productivity (Barnett et al., 2005; Ohmura and Wild, 2002).

Changes in sublimation losses associated with climate warming may have important hydrologic impacts. In this regard, it is necessary to consider how available energy is partitioned between sensible and latent heat fluxes. Relative to the control simulations, heated and NM SNOWPACK simulations consistently estimated greater proportions of energy associated with latent heat flux (Table 2), which is consistent with results from Molotch et al. (2009). This increased latent heat flux in heated plots resulted in a 230% and 112% increase in sublimation rates versus control plots during the accumulation and melt periods, respectively. The direction of these changes were consistent with model results from the

NM site and from previous works (Molotch et al., 2009) indicating that water availability may be reduced significantly in warmer conditions. Interestingly, this same effect was not seen as strongly in the synthetic simulation, raising a question as to whether NM is a sufficient analog for a warmer CO when considering turbulent fluxes.

While using IR heaters in snow-dominated systems have limitations, alternative experimental warming techniques have their own advantages and drawbacks. Open top chamber experiments are an attractive alternative in mountainous settings as they do not require electricity but these techniques significantly alter snowpack structure as the chambers effectively fill with snow in high wind environments (Bokhorst et al., 2013). Manipulation of snow surface albedo through the addition of light absorbing impurities (e.g. Blankinship et al., 2014) represents an alternative approach but this technique does not alter surface energy fluxes once snow has disappeared; i.e. the technique is only useful for snow manipulation. This technique is also of limited utility in densely forested environments where sub-canopy solar irradiance is low relative to alpine settings. Mechanical removal or addition of snow (e.g. Cornelius et al., 2013) represents another alternative but this technique is highly destructive to the snowpack stratigraphy and therefore fluxes of energy and water vapor within the snowpack will become unrealistic. The IR heater technique is quite attractive from the standpoint of preserving snow microstructure and evaluating the response of snow properties to changes in the surface energy balance. As non-destructive snow measurement techniques develop (e.g. Marshall and Koh, 2008; Berisford et al., 2013), future works will be able to directly observe the impacts of IR heating on snow microstructure. Notwithstanding, IR heaters also have drawbacks with regard to snow microstructure and snow–atmosphere energy exchange. IR heaters may induce changes in turbulent fluxes which are unrealistic in magnitude and opposite in sign. For example, the heaters may raise the snow surface temperature to 0 °C when the air temperature remains well below 0 °C. As a result, the temperature gradient between the snow and overlying atmosphere can reverse sign and/or increase in magnitude relative to control conditions. This scenario is observed in Fig. 11 where the 2010 heated case is the only simulation with a negative sensible heat flux while the control simulation has a positive sensible heat flux with a smaller magnitude.

IR heaters may also induce unexpected changes to net shortwave radiation, as heaters effect the snow-surface grain size and therefore the snow albedo. These changes can have differential impacts on net shortwave radiation depending on the timing of snowmelt. In this context, modeled differential net shortwave responses to heating between 2011 and 2012 may have resulted from differences in the timing of modeled snowmelt and associated differences in solar zenith angles. For example, snow disappearance in heated plots occurred over 70 days later in 2011 versus 2012 and therefore melt simulations in heated plots in 2011 occurred when solar elevations and solar irradiance were greater. The timing of snowfall events can complicate these effects as differences in snow surface grain size between control and heated plots may be more significant after snowfall events; i.e. because heaters cause increased grain growth rates. Hence, if snowfall events occur in spring, when inter-storm solar zenith angles are relatively low, heated plots may have disproportionately greater net solar radiation versus control plots. This may have occurred in 2011, as late spring snowfall events were more common than 2012 (Figs. 4 and 8). Given albedo measurements were not taken over heated plots, we cannot accurately quantify the magnitude of these effects; deployment of albedometers over heated and control plots is recommended for future research.

Considering the NM site as an approximate benchmark for future winter climate at the CO site, the 2010 heater level of 50% maximum power was too high to produce a realistic future snowpack projection. Conversely, the mid-winter heater output in 2011 of 10% maximum power was too low. Heater settings in 2012 (10–40% of maximum power) resulted in a similar snowpack to that of NM, and thus a heater setting of 10–20% mid-winter and 40% during the spring melt season (or 42–85 and 171 W m^2) seems to produce a realistic snowpack manipulation for a targeted warming of ~4 °C. A second design consideration for IR heaters and snow-climate manipulation experiments is that the snow persisted longer in the center of the heated plots (Fig. 2b) creating an annulus snow ablation pattern and resulting in manual versus digital measurement discrepancies. Consideration of the annulus in the context of the results presented here is difficult to do in a quantitative manner as we did not have manual measurements of snow depth within the plots. Making such measurements would disturb the soils within the plots and could potentially compromise ecological experiments within the plots by limiting seedling survival. As such, one can only take the snow depth observations here as the upper bound of snow depth within the heated plots. Hence, the heated simulation under-estimates in snow depth during spring of 2011 may be exaggerated as presented in Fig. 4. Despite Kimball et al. (2008) optimized IR heater array design, different considerations may need to be taken for future IR experiments involving snow. For instance, a smaller plot diameter or maintaining heater elevation at 1.2 m above the snow surface may be more suitable to produce spatially uniform heating of snow with IR heaters. In addition, more advanced methods of snow depth monitoring within the plots could be employed; for example, using terrestrial laser scanning (Prokop, 2008).

It is important to note that using SWE observations, rather than snow depth observations, would be a more robust method for comparing the snow conditions under the different scenarios. Comparisons with observed SWE were not possible because SWE was not observed continuously at the sites. In addition, SWE measurements were not possible inside the heated plots because SWE is a destructive measurement and the snow must remain pristine inside the plots. Using snow depth as a proxy for SWE may be problematic as it is not possible to decipher snow densification and sublimation losses from snowmelt when observing the snow depth time series. Earlier works have documented differential rates of densification (Musselman et al., 2008) and sublimation (Gustafson et al., 2010) over small spatial scales (<5 m) in forested environments and therefore relationships between depth and SWE are highly variable which limits the utility of snow depth as a proxy for SWE. Notwithstanding, if we focus on the control simulations with respect to gaining confidence in the model, it is apparent that the model tends to represent the upper end of observed snow depth observations (Fig. 4). Snow density observations near control plots indicate that the model tended to underestimate snow density. Hence, errors in modeled SWE are likely lower than the errors in snow depth shown in Fig. 4; i.e. because SWE represents the product of depth (slightly over-estimated) and density (i.e. slightly under-estimated).

The model biases shown in Fig. 4 may be a result of uncertainty in model structure and/or model forcings. With regard to model structure, several studies using SNOWPACK have documented a systematic overestimation of SWE and underestimation of melt rates (Bartelt and Lehning, 2002), underestimation of snowpack settling (Lundy et al., 2001), and greater error tendency as a snow cover becomes isothermal at 0 °C (Lundy et al., 2001; Rasmus et al., 2004; Yamaguchi et al., 2004). With regard to forcings, the SNOWPACK canopy module treats the forest canopy as a single large leaf with input parameters of canopy height, leaf-area index (LAI), and direct throughfall fraction, and incoming radiation is attenuated using a Beer–Lambert Law approximation (Musselman et al., 2012). However, the Beer–Lambert law application has been shown

to be insufficient for resolving sub-canopy irradiance for sub-daily timescales (Reifsnyder et al., 1971), and therefore model biases presented here may have resulted from inadequate treatment of forest radiative transfer.

With regard to precipitation forcing, the observed over-catch at our measurement site is a bit perplexing as many previous works have noted a tendency for precipitation under-catch in locations where snowfall is the dominant form of precipitation. Precipitation over-catch has been documented in the literature as a result of blowing snow (Li and Pomeroy, 1997; Struzer, 1971; UNESCO, 1978; Benning and Yang, 2005; Williams et al., 1998a,b; Yang et al., 2000; Yang and Ohata, 2001) and unloading of canopy intercepted snow (Clagett, 1988). With regard to unloading of intercepted snow, Clagett (1988) hypothesized that precipitation reference sites in small forest clearings over-catch blowing and unloading snow from nearby canopies. In addition, small clearings in forests can over-catch precipitation due to changes in the turbulent regimes created by the clearings. Golding and Swanson (1978) observed approximately 36% greater snow accumulation in forest clearings that were roughly equivalent in size to the canopy height. Less than half of the increased precipitation could be attributed to the absence of interception by the tree canopy, suggesting that changes in turbulence over the forest canopy led to increased deposition in the clearing. While we cannot determine the exact cause of the precipitation over-catch at our site, the proximity of the canopy to the precipitation gauge (i.e. ~10 m), the size of the gap dimension (i.e. on the order of the tree height), and the relatively high above-canopy wind speeds, likely creates conditions favorable for gauge over-catch.

8. Conclusions

Relative to control plots, heated plots experienced 30% lower observed snow depth, an estimated 51% less modeled SWE, and 2 weeks earlier snow disappearance. These results were generally consistent with the naturally warmer New Mexico site, which had 23% lower observed snow depth, 42% less modeled SWE, and 3 weeks earlier snow disappearance. Relative to control simulations, heated and New Mexico simulations exhibited larger snow grain sizes and greater snow temperature. Both the heated and NM simulations indicate changes to energy partitioning associated with warmer climatic conditions. Greater latent heat fluxes and sublimation water losses during both accumulation and melt seasons were simulated with Q_e accounting for 6% of energy exchange for control simulations and 21% in the NM and synthetic simulations. Average sublimation rates for control simulations were 59% and 71% lower than in heated and NM simulations, respectively. These observed and modeled differences in snowpack, soil dynamics, and energy exchange may have dramatic hydrological and ecological consequences; both within IR warming plots and broadly across the landscape. The work presented herein illustrates that snowpack accumulation and snowmelt response to IR heaters generally falls within realistic bounds. Alterations to snowpack-atmosphere energy exchange and associated sublimation may result in unintended manipulation of the soil water budget. IR heaters represent a viable option for climate manipulation in snow covered ecosystems but extreme care must be taken regarding the level of heater output, heater distance from the snow surface, and augmentation of the soil water budget due to sublimation losses.

Acknowledgements

This research was supported by NASA grants NNX08AH18G, NNX11AK35A, NSF grants EAR 1032295, EAR 1141764, USDA grant 2012-67003-19802, the NOAA RISA Western Water Assessment, U.S. Department of Energy, Office of Science (BER), and the NSF Niwot Ridge Long Term Ecological Research program. Darin Desilets Marcy Litvak, Jen Petrzelka, Michi Lehning, Danielle Perrot, Dominik Schneider, Scott Ferrenberg, and Ethan Brown are acknowledged for providing data sets and field and technical support.

References

Adam, J.C., Hamlet, A.F., Lettenmaier, D.P., 2009. Implications of global climate change for snowmelt hydrology in the twenty-first century. Hydrol. Process. 23 (7), 962–972.
Amthor, J.S., Hanson, P.J., Norby, R.J., Wullschleger, S.D., 2010. A comment on "Appropriate experimental ecosystem warming methods by ecosystem, objective, and practicality" by Aronson and McNulty. Agric. Forest Meteorol. 150 (3), 497–498.
Aronson, E.L., McNulty, S.G., 2009. Appropriate experimental ecosystem warming methods by ecosystem, objective, and practicality. Agric. Forest Meteorol. 149 (11), 1791–1799.
Auyeung, D.S.N., Suseela, V., Dukes, J.S., 2013. Warming and drought reduce temperature sensitivity of nitrogen transformations. Glob. Change Biol. 19, 662–676.
Bales, R.C., Molotch, N.P., Painter, T.H., Dettinger, M., Rice, R., Dozier, J., 2006. Mountain hydrology of the western United States. Water Resour. Res. 42 (8), http://dx.doi.org/10.1029/2005WR004387.
Barnett, T.P., Adam, J.C., Lettenmaier, D.P., 2005. Potential impacts of a warming climate on water availability in snow-dominated regions. Nature 438 (7066), 303–309.
Bartelt, P., Lehning, M., 2002. A physical SNOWPACK model for the Swiss avalanche warning. Part I. Numerical model. Cold Reg. Sci. Technol. 35 (3), 123–145.
Bavay, M., Lehning, M., Jonas, T., Lowe, H., 2009. Simulations of future snow cover and discharge in Alpine headwater catchments. Hydrol. Process. 23 (1), 95–108.
Beniston, M., Keller, F., Koffi, B., Goyette, S., 2003. Estimates of snow accumulation and volume in the Swiss Alps under changing climatic conditions. Theor. Appl. Climatol. 76 (3–4), 125–140.
Benning, J., Yang, D., 2005. Adjustment of daily precipitation data at barrow and Nome Alaska for 1995–2001. Arct. Antarct. Alp. Res. 37 (August (3)), 276–283.
Berisford, D.F., Molotch, N.P., Durand, M.T., Painter, T.H., 2013. Portable spectral profiler probe for rapid snow grain size stratigraphy. Cold Reg. Sci. Technol. 85, 183–190, http://dx.doi.org/10.1016/j.coldregions.2012.09.007.
Blanken, P.D., et al., 2009. A comparison of water and carbon dioxide exchange at a windy alpine tundra and subalpine forest site near Niwot Ridge, Colorado. Biogeochemistry 95 (1), 61–76.
Blankinship, J.C., Meadows, M.W., et al., 2014. Snowmelt timing alters shallow but not deep soil moisture in the Sierra Nevada. Water Resour. Res. 50 (2), 1448–1456.
Bokhorst, S., Huiskes, A., Aerts, R., et al., 2013. Variable temperature effects of open top chambers at polar and alpine sites explained by irradiance and snow depth. Glob. Change Biol. 19, 64–74.
Brooks, P.D., Grogan, P., Templer, P.H., Groffman, P., Öquist, M.G., Schimel, J., 2011. Carbon and nitrogen cycling in snow-covered environments. Geogr. Compass 5, 682–699, http://dx.doi.org/10.1111/j.1749-8198.2011.00420.x.
Caine, N., 1995. Temporal trends in the quality of streamwater in an Alpine environment: Green Lakes valley, Colorado Front Rand, USA. Geogr. Ann. Ser. A-Phys. Geogr. 77A (4), 207–220.
Campbell, J.L., Mitchell, M.J., Groffman, P.M., Christenson, L.M., Hardy, J.P., 2005. Winter in northeastern North America: a critical period for ecological processes. Front. Ecol. Environ. 3 (6), 314–322.
Castanha, C., Torn, M.S., Germino, M.J., Weibel, B., Kueppers, L.M., 2013. Conifer seedling recruitment across a gradient from forest to alpine tundra: effects of species, provenance, and site. Plant Ecol. Divers. 6, 307–318.
Clagett, G.P., 1988. The Wyoming shield – an evaluation after 12 years use in Alaska. In: Proceedings of the Western Snow Conference, Kalispell, Montana, pp. 113–123.
Clow, D.W., 2010. Changes in the timing of snowmelt and streamflow in Colorado: a response to recent warming. J. Clim. 23 (9), 2293–2306.
Comerford, D., Schaberg, P., Templer, P., Socci, A., Campbell, J., Wallin, K., 2013. Influence of experimental snow removal on root and canopy physiology of sugar maple trees in a northern hardwood forest. Oecologia 171, 261–269.
Cornelius, C., Leingärtner, A., Hoiss, B., Krauss, J., Steffan-Dewenter, I., Menzel, A., 2013. Phenological response of grassland species to manipulative snowmelt and drought along an altitudinal gradient. J. Exp. Bot. 64 (1), 241–251, http://dx.doi.org/10.1093/jxb/ers321.
Decker, K.L.M., Wang, D., Waite, C., Scherbatskoy, T., 2003. Snow removal and ambient air temperature effects on forest soil temperatures in Northern Vermont. Soil Sci. Soc. Am. J. 67, 1234–1242.
Deems, J.S., Painter, T.H., Barsugli, J.J., Belnap, J., Udall, B., 2013. Combined impacts of current and future dust deposition and regional warming on Colorado River Basin snow dynamics and hydrology. Hydrol. Earth Syst. Sci. 17 (11), 4401–4413, http://dx.doi.org/10.5194/hess-17-4401-2013.

Desilets, D., Zreda, M., Ferre, T.P.A., 2010. Nature's neutron probe: land surface hydrology at an elusive scale with cosmic rays. Water Resour. Res. 46, http://dx.doi.org/10.1029/2009wr008726.
Dunne, J.A., Harte, J., Taylor, K.J., 2003. Subalpine meadow flowering phenology responses to climate change: integrating experimental and gradient methods. Ecol. Monogr. 73, 69–86.
Essery, R., Pomeroy, J., Parviainen, J., Storck, P., 2003. Sublimation of snow from coniferous forests in a climate model. J. Clim. 16, 1855–1864, http://dx.doi.org/10.1175/1520-0442(2003)016<1855:SOSFCF>2.0.CO;2.
Filippa, G., et al., 2009. Winter and summer nitrous oxide and nitrogen oxides fluxes from a seasonally snow-covered subalpine meadow at Niwot Ridge, Colorado. Biogeochemistry 95 (1), 131–149.
Flanner, M.G., Shell, K.M., Barlage, M., Perovich, D.K., Tschudi, M.A., 2011. Radiative forcing and albedo feedback from the Northern Hemisphere cryosphere between 1979 and 2008. Nat. Geosci. 4, 151–155, http://dx.doi.org/10.1038/ngeo1062.
Franco, B., Fettweis, X., Erpicum, M., 2013. Future projections of the Greenland ice sheet energy balance driving the surface melt. Cryosphere 7 (1), 1–18.
Gillan, B.J., Harper, J.T., Moore, J.N., 2010. Timing of present and future snowmelt from high elevations in northwest Montana. Water Resour. Res. 46, 13.
Golding, D.L., Swanson, R.H., 1978. Snow accumulation and melt in small forest openings in Alberta. Can. J. Forest Res. 8, 380–388.
Goodison, B.E., Louie, P.Y.T., Yang, D., 1998. WMO Solid Precipitation Measurement Intercomparison. Final Report, WMO/TD-No. 872., pp. 212.
Goodison, B.E., 1981. Compatibility of Canadian snowfall and snowcover data. Water Resour. Res. 17 (4), 893–900.
Groffman, P.M., et al., 2001. Colder soils in a warmer world: a snow manipulation study in a northern hardwood forest ecosystem. Biogeochemistry 56 (2), 135–150.
Gustafson, J.R., Brooks, P.D., Molotch, N.P., Veatch, W.C., 2010. Estimating snow sublimation using natural chemical and isotopic tracers across a gradient of solar radiation. Water Resour. Res. 46, http://dx.doi.org/10.1029/2009WR009060.
Hamlet, A.F., Mote, P.W., Clark, M.P., Lettenmaier, D.P., 2005. Effects of temperature and precipitation variability on snowpack trends in the western United States. J. Clim. 18 (21), 4545–4561.
Hamlet, A.F., Mote, P.W., Clark, M.P., Lettenmaier, D.P., 2007. Twentieth-century trends in runoff, evapotranspiration, and soil moisture in the western United States. J. Clim. 20 (8), 1468–1486.
Harte, J., Shaw, R., 1995. Shifting dominance within a montane vegetation community – results of a climate-warming experiment. Science 267 (5199), 876–880.
Harte, J., Torn, M., Chang, F.-R., Feifarek, B., Kinzig, A., Shaw, R., Shen, K., 1995. Global warming and soil microclimate: Results from a meadow-warming experiment. Ecol. Appl. 5, 132–150.
IPCC, 2007. Climate Change 2007: Working Group 1: The Physical Science Basics, Summary for Policymakers, Intergovernmental Panel on Climate Change. Cambridge University Press, Geneva, Switzerland.
Kimball, B.A., 2005. Theory and performance of an infrared heater for ecosystem warming. Glob. Change Biol. 11 (11), 2041–2056.
Kimball, B.A., et al., 2008. Infrared heater arrays for warming ecosystem field plots. Glob. Change Biol. 14 (2), 309–320.
Kimball, B.A., 2011. Comment on the comment by Amthor et al. on "Appropriate experimental ecosystem warming methods" by Aronson and McNulty. Agric. Forest Meteorol. 151 (3), 420–424.
Lapp, S., Byrne, J., Townshend, I., Kienzle, S., 2005. Climate warming impacts on snowpack accumulation in an alpine watershed. Int. J. Climatol. 25 (4), 521–536.
Lehning, M., Bartelt, P., Brown, B., Fierz, C., 2002a. A physical SNOWPACK model for the Swiss avalanche warning. Part III. Meteorological forcing, thin layer formation and evaluation. Cold Reg. Sci. Technol. 35 (3), 169–184.
Lehning, M., Bartelt, P., Brown, B., Fierz, C., Satyawali, P., 2002b. A physical SNOWPACK model for the Swiss avalanche warning. Part II. Snow microstructure. Cold Reg. Sci. Technol. 35 (3), 147–167.
Li, L., Pomeroy, J.W., 1997. Estimates of threshold wind speeds for snow transport using meteorological data. J. Clim. Appl. Meteorol. 36, 205–213.
Link, T.E., Marks, D., 1999. Point simulation of seasonal snow cover dynamics beneath boreal forest canopies. J. Geophys. Res. Atmos. 104 (D22), 27841–27857.
Loik, M.E., Griffith, A.B., Alpert, H., 2013. Impacts of long-term snow climate change on a high-elevation cold desert shrubland, California, USA. Plant Ecol. 214 (2), 255–266.
Lopez-Moreno, J.I., Goyette, S., Beniston, M., 2009. Impact of climate change on snowpack in the Pyrenees: horizontal spatial variability and vertical gradients. J. Hydrol. 374 (3–4), 384–396.
Lopez-Moreno, J.I., Goyette, S., Beniston, M., Alvera, B., 2008. Sensitivity of the snow energy balance to climatic changes: prediction of snowpack in the Pyrenees in the 21st century. Clim. Res. 36 (3), 203–217.
Lundquist, J.D., Flint, A.L., 2006. Onset of snowmelt and streamflow in 2004 in the western United States: how shading may affect spring streamflow timing in a warmer world. J. Hydrometeorol. 7 (6), 1199–1217.
Lundy, C.C., Brown, R.L., Adams, E.E., Birkeland, K.W., Lehning, M., 2001. A statistical validation of the snowpack model in a Montana climate. Cold Reg. Sci. Technol. 33 (2–3), 237–246.
Magnusson, J., Jonas, T., Lopez-Moreno, I., Lehning, M., 2010. Snow cover response to climate change in a high alpine and half-glacierized basin in Switzerland. Hydrol. Res. 41 (3–4), 230–240.
Male, D.H., Granger, R.J., 1981. Snow surface-energy exchange. Water Resour. Res. 17 (3), 609–627.
Marshall, H.P., Koh, G., 2008. FMCW radars for snow research. Cold Reg. Sci. Technol. 52 (2), 118–131.
McClung, D.M., Schaerer, P., 2006. The Avalanche Handbook. The Mountaineers (pub.), Seattle, pp. 342.
McDowell, N.G., White, S., Pockman, W.T., 2008. Transpiration and stomatal conductance across a steep climate gradient in the southern Rocky Mountains. Ecohydrology 1 (3), 193–204.
Molotch, N.P., Blanken, P.D., Williams, M.W., Turnipseed, A.A., Monson, R.K., Margulis, S.A., 2007. Estimating sublimation of intercepted and sub-canopy snow using eddy covariance systems. Hydrol. Process. 21, http://dx.doi.org/10.1002/hyp.6719.
Molotch, N.P., Brooks, P.D., Burns, S.P., Litvak, M., McConnell, J.R., Monson, R.K., Musselman, K., 2009. Ecohydrological controls on snowmelt partitioning in mixed-conifer sub-alpine forests. Ecohydrology 2 (2), 129–142, http://dx.doi.org/10.1002/eco.48.
Monson, R.K., Lipson, D.L., Burns, S.P., Turnipseed, A.A., Delany, A.C., Williams, M.W., Schmidt, S.K., 2006. Winter forest soil respiration controlled by climate and microbial community composition. Nature 439, 711–714, http://dx.doi.org/10.1038/nature04555.
Mote, P.W., Hamlet, A.F., Clark, M.P., Lettenmaier, D.P., 2005. Declining mountain snowpack in western North America. Bull. Am. Meteorol. Soc. 86 (1), 39–49.
Moyes, A.B., Castanha, C., Germino, M.J., Kueppers, L.M., 2013. Warming and the dependence of limber pine (*Pinus flexilis*) establishment on summer soil moisture within and above its current elevation range. Oecologia 171 (1), 271–282.
Musselman, K.N., Molotch, N.P., Margulis, S.A., Lehning, M., Gustafsson, D., 2012. Improved snowmelt simulations with a canopy model forced with photo-derived direct beam canopy transmissivity. Water Resour. Res. 48, http://dx.doi.org/10.1029/2012WR012285.
Musselman, K., Molotch, N.P., Brooks, P.D., 2008. Effects of vegetation on snow accumulation and ablation in a mid-latitude sub-alpine forest. Hydrol. Process. 22, 2767–2776, http://dx.doi.org/10.1002/hyp.7050.
Ohmura, A., Wild, M., 2002. Is the hydrological cycle accelerating? Science 298 (5597), 1345–1346.
Pagano, T., Garen, D., 2005. A recent increase in western US streamflow variability and persistence. J. Hydrometeorol. 6 (2), 173–179.
Prokop, A., 2008. Assessing the applicability of terrestrial laser scanning for spatial snow depth measurements. Cold Reg. Sci. Technol. 54 (3), 155–163, http://dx.doi.org/10.1016/j.coldregions.2008.07.002.
Rasmus, S., Raisanen, J., Lehning, M., 2004. Estimating snow conditions in Finland in the late 21st century using the SNOWPACK model with regional climate scenario data as input. In: Fohn, P.M.B. (Ed.), Annals of Glaciology, vol. 38, pp. 238–244.
Rasmussen, R., Ikeda, K., Liu, C., Gochis, D., Clark, M., Dai, A., Gutmann, E., Dudhia, J., Chen, F., Barlage, M., Yates, D., Zhang, G., 2014. Climate change impacts on the water balance of the Colorado headwaters: high-resolution regional climate model simulations. J. Hydrometeorol. 15, 1091–1116, http://dx.doi.org/10.1175/JHM-D-13-0118.1.
Rauscher, S.A., Pal, J.S., Diffenbaugh, N.S., Benedetti, M.M., 2008. Future changes in snowmelt-driven runoff timing over the western US. Geophys. Res. Lett. 35 (16).
Reifsnyder, W.E., Furnival, G.M., Horowitz, J.L., 1971. Spatial and temporal distribution of solar radiation beneath forest canopies. Agric. Meteorol. 9 (1–2), 21.
Schulz, O., de Jong, C., 2004. Snowmelt and sublimation: field experiments and modelling in the High Atlas Mountains of Morocco. Hydrol. Earth Syst. Sci. 8 (6), 1076–1089 (Discussions).
Small, E.E., McConnell, J.R., 2008. Comparison of soil moisture and meteorological controls on pine and spruce transpiration. Ecohydrology 1 (3), 205–214.
Stewart, I.T., Cayan, D.R., Dettinger, M.D., 2004. Changes in snowmelt runoff timing in western North America under a 'business as usual' climate change scenario. Clim. Change 62 (1–3), 217–232.
IPCC, 2013. Summary for policymakers. In: Stocker, T.F., Qin, D., Plattner, G.-K., Tignor, M., Allen, S.K., Boschung, J., Nauels, A., Xia, Y., Bex, V., Midgley, P.M. (Eds.), Climate Change 2013: The Physical Science Basis. Contribution of Working Group I to the Fifth Assessment Report of the Intergovernmental Panel on Climate Change. Cambridge University Press, Cambridge, United Kingdom/New York, NY, USA.
Struzer, I.R., 1971. On the ways of account of precipitation gage errors caused by falling of false precipitation into precipitation gage during blizzards. Trans. Main Geophys. Obs. 260, 35–60.
Trujillo, E., Molotch, N.P., Goulden, M.L., Kelly, A.E., Bales, R.C., 2012. Elevation-dependent influence of snow accumulation on forest greening. Nat. Geosci. 5 (10), 705–709, http://dx.doi.org/10.1038/ngeo1571.
Turnipseed, A.A., Anderson, D.E., Blanken, P.D., Baugh, W.M., Monson, R.K., 2003. Airflows and turbulent flux measurements in mountainous terrain Part 1. Canopy and local effects. Agric. Forest Meteorol. 119 (1–2), 1–21.
UNESCO, 1978. World water balance and water resources of the earth. Studies and Reports in Hydrology, vol. 25. UNESCO, Paris, pp. 663.
Vicuna, S., Garreaud, R.D., McPhee, J., 2011. Climate change impacts on the hydrology of a snowmelt driven basin in semiarid Chile. Clim. Change 105 (3–4), 469–488.
Walker, M.D., et al., 1999. Long-term experimental manipulation of winter snow regime and summer temperature in arctic and alpine tundra. Hydrol. Process. 13 (14–15), 2315–2330.
Wall, G.W., Kimball, B.A., White, J.W., Ottman, M.J., 2011. Gas exchange and water relations of spring wheat under full-season infrared warming. Glob. Change Biol. 17, 2113–2133, http://dx.doi.org/10.1111/j.1365-2486.2011.02399.x.

Wan, S., Luo, Y., Wallace, L.L., 2002. Changes in microclimate induced by experimental warming and clipping in tallgrass prairie. Glob. Change Biol. 8 (8), 754–768.
Westerling, A.L., Hidalgo, H.G., Cayan, D.R., Swetnam, T.W., 2006. Warming and earlier spring increase western US forest wildfire activity. Science 313 (5789), 940–943.
Williams, M.W., Brooks, P.D., Seastedt, T., 1998a. Nitrogen and carbon soil dynamics in response to climate change in a high-elevation ecosystem in the Rocky Mountains, USA. Arct. Alp. Res. 30 (1), 26–30.
Williams, M.W., Bardsley, T., Rikkers, M., 1998b. Oversampling of snow and overestimation of inorganic nitrogen wetfall using NADP data, Niwot Ridge, Colorado. Atmos. Environ. 32 (22), 3827–3833.
Wipf, S., Rixen, C., 2010. A review of snow manipulation experiments in Arctic and alpine tundra ecosystems. Polar Res. 29 (1), 95–109.
Wu, Z., Dijkstra, P., Koch, G.W., Penuelas, J., Hungate, B.A., 2011. Responses of terrestrial ecosystems to temperature and precipitation change: a meta-analysis of experimental manipulation. Glob. Change Biol. 17, 927–942.
Yamaguchi, S., Sato, A., Lehning, M., 2004. Application of the numerical snowpack model (SNOWPACK) to the wet-snow region in Japan. Annals of Glaciology, vol. 38, pp. 266–272(7).
Yang, D., Ohata, T., 2001. A bias-corrected siberian regional precipitation climatology. J. Hydrometeorol. 2, 122–139, http://dx.doi.org/10.1175/1525-7541(2001)002<0122:ABCSRP>2.0.CO;2.
Yang, D., Kane, D.L., Hinzman, L.D., Goodison, B.E., Metcalfe, J.R., Louie, P.Y.T., Leavesley, G.H., Emerson, D.G., Hansons, C.L., 2000. An evaluation of the Wyoming gauge system for snowfall measurement. Water Resour. Res. 36 (9), 2665–2677.